



Universiteit
Leiden
The Netherlands

Fragmentation of the PAH cations of Isoviolanthrene and Dicoronylene: a case made for interstellar cyclo[n]carbons as products of universal fragmentation processes

Hrodmarsson, H.R.; Bouwman, J.; Tielens, A.G.G.M.; Linnartz, H.V.J.

Citation

Hrodmarsson, H. R., Bouwman, J., Tielens, A. G. G. M., & Linnartz, H. V. J. (2023). Fragmentation of the PAH cations of Isoviolanthrene and Dicoronylene: a case made for interstellar cyclo[n]carbons as products of universal fragmentation processes. *International Journal Of Mass Spectrometry*, 485. doi:10.1016/j.ijms.2022.116996

Version: Publisher's Version

License: [Creative Commons CC BY 4.0 license](https://creativecommons.org/licenses/by/4.0/)

Downloaded from: <https://hdl.handle.net/1887/3719518>

Note: To cite this publication please use the final published version (if applicable).



Fragmentation of the PAH cations of Isovioanthrene and Dicoronylene: A case made for interstellar cyclo[*n*]carbons as products of universal fragmentation processes



Helgi Rafn Hrodmarsson^{a,*}, Jordy Bouwman^{b,c,d}, Alexander G.G.M. Tielens^e, Harold Linnartz^a

^a Laboratory for Astrophysics, Leiden Observatory, Leiden University, PO Box 9513, NL-2300 RA Leiden, the Netherlands

^b Laboratory for Atmospheric and Space Physics, University of Colorado, Boulder, CO, 80303, USA

^c Department of Chemistry, University of Colorado, Boulder, CO, 80309, USA

^d Institute for Modeling Plasma, Atmospheres, and Cosmic Dust (IMPACT), University of Colorado, Boulder, CO, 80303, USA

^e Leiden Observatory, Leiden University, PO Box 9513, NL-2300 RA Leiden, the Netherlands

ARTICLE INFO

Article history:

Received 21 July 2022

Received in revised form

6 December 2022

Accepted 7 December 2022

Available online 8 December 2022

ABSTRACT

The photo-induced fragmentation pathways of the cationic forms of isovioanthrene (C₃₄H₁₈) and dicoronylene (C₄₈H₂₀) are systematically studied with mass spectrometry employing an ion trap coupled with a laser system. The mass spectra of these structurally different species display similar fragmentation products, akin to previous work on three dibenzopyrene isomers, but also display some differences. The products formed in the largest yields are pure carbon clusters, which are likely in the form of ionized cyclo[*n*]carbons (*n* = 11–15). These findings are relevant to get a full picture of the molecular makeup of interstellar space, particularly in heavily irradiated regions where polycyclic aromatic hydrocarbon (PAH) molecules are omnipresent and subject to harsh irradiation and are broken down into smaller components. These interstellar species are expected to include the PAH derivatives observed here, but which are not identified in space yet.

© 2022 The Authors. Published by Elsevier B.V. This is an open access article under the CC BY license (<http://creativecommons.org/licenses/by/4.0/>).

1. Introduction

By now it is well established that the strongest mid-IR emission features dominating the spectra of galactic and extragalactic sources originate from large polycyclic aromatic hydrocarbons (PAHs) [1–3]. With the recent molecule specific identifications of several PAHs in cold molecular clouds [4–6], the aromaticity of our universe is uncontested. PAHs are furthermore theorized to comprise up to 15% of the galactic carbon budget [7,8] and are now used to trace star-forming galaxies and active galactic nuclei regions [9,10]. While PAHs are expected to form in the stellar outflows of carbon-rich stars [11], mainly large, compact, and symmetric (GRAND)PAHs are predicted to survive the harsh ISM conditions [12]. This makes them likely carriers of the mid-IR emission features in various interstellar environments [13]. The GRANDPAH hypothesis states

that a limited number of compact, highly symmetric PAHs dominate the interstellar PAH family at the brightest spots of photon-rich regions and that the other (less symmetric) PAHs fragment, enriching the ISM with aromatic debris. For this reason, it is not only important to focus on PAHs of astronomical relevance themselves, but also on their fragmentation behavior and the resulting products.

Many prior studies have focused on PAH fragmentation [14–23] and in very recent work from our group [24] we showed how three dibenzopyrene (C₂₄H₁₄) isomers with clearly different geometries exhibit very similar fragmentation behaviors. We showed that under laser irradiation, C_{*n*}⁺ (*n* = 11–15) carbon clusters are preferentially formed in similar branching ratios. Here, we expand on these findings, applying the same methodology with a focus on larger and geometrically different PAH molecules, namely isovioanthrene and dicoronylene (see Fig. 1) with the aim to look for similarities and differences in fragmentation behavior compared to the dibenzopyrenes.

* Corresponding author.

E-mail addresses: hrodmarsson@strw.leidenuniv.nl, hr.hrodmarsson@gmail.com (H.R. Hrodmarsson).

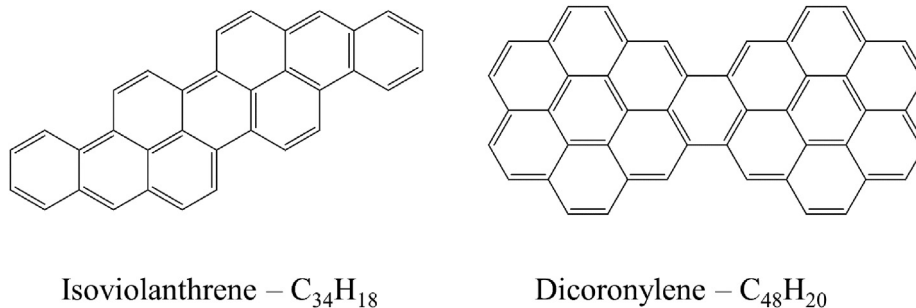


Fig. 1. Chemical structures and formulas for the PAHs considered in this work.

2. Methods

The experiments were performed on the ‘instrument for Photodynamics of PAHs’ (i-PoP), situated in the Laboratory for Astrophysics (LfA) at Leiden Observatory. i-PoP has been described in detail elsewhere [23] and the experimental methodology and analysis were detailed previously [24] so only a brief description is given here. The apparatus consists of two differentially pumped chambers; a source chamber that houses a commercially available ion trap (Jordan C-1251), and a detection chamber which comprises a reflectron time-of-flight mass spectrometer (Jordan D-850). The samples were evaporated in the source chamber using a Heat Wave Labs oven. Isoviolanthrene was sublimated at 150 °C and dicoronylene at 300 °C. The samples were ionized by an electron gun (EGUN, Jordan C-950) using 70 eV electrons, and guided into the ion trap. The ion trap was filled with a He buffer gas up to a standard backing pressure of $1\text{--}2 \times 10^{-6}$ mbar. The contents of the ion trap were irradiated with a dye laser (LiopStar) running at DCM dissolved in ethanol and pumped by a nanosecond pulsed Quanta-Ray Nd:YAG laser (DCR2A-3235) and delivering 620 nm photons. This choice of photon wavelength enabled us to simultaneously bypass multiple ionization and investigate the potential energy surface in a gentler manner than by using more energetic photons. The laser was guided horizontally through the ion trap and operated at 10 Hz to irradiate the trapped ions. The timing sequences of the data acquisition cycle were controlled by a high-precision delay generator (SRS DG535). To isolate the masses of the parent PAH ions before laser exposure a *ca.* 200 ms long SWIFT pulse [25] was applied to the end caps of the ion. After the SWIFT pulse was employed, the laser beam shutter was opened, and the ion cloud irradiated. At the end of the irradiation time, the ions were accelerated out of the trap and into the field-free TOF region at the end of which the ions were detected by a microchannel plate.

Several data acquisitions were performed where the laser power was varied as well as the number of laser pulses to explore the photofragmentation process as a function of both variables. So-called acquisition ‘trains’ were performed with 4.0 and 6.5 mJ energies per laser pulse (or 40 and 65 mJ/cm²/pulse, respectively) with the following numbers of pulses: 1, 2, 3, 4, 5, 10, 15, and 20. In each measurement, the total duration of a measurement cycle was kept constant at 5 s to ensure cross compatibility of our measurements. In the next sections, data are presented in the form of TOF-MS matrices whose construction was described in detail previously [24]. In short, these diagrams not only show mass signals (*m/z*) but also the intensity in dependence of the number of applied laser pulses for a specific mass. In the same reference, detailed information on the data treatment and analysis is given.

3. Results

3.1. Mass spectra

The TOF-MS matrices of isoviolanthrene and dicoronylene are presented in Figs. 2 and 3, respectively. Two matrices corresponding to different laser pulse train energies (namely 4.0 and 6.5 mJ/pulse in upper and lower panel, respectively) are presented in each case.

For isoviolanthrene (Fig. 2), there are many similarities with the three dibenzopyrene isomers studied previously [24]. On the surface, this seems reasonable, at least for the case of dibenzo[a,h]pyrene whose carbon skeleton blueprint is embedded within the molecular structure of isoviolanthrene. Like the dibenzopyrenes, isoviolanthrene does not completely dehydrogenate before losing carbon atoms from its structure. This can be observed in both panels between 1 and 5 laser pulses, where there are clear signals corresponding to C₂(H₂) loss followed by subsequent dehydrogenation or from a partially dehydrogenated parent. It is worth noting that as in our previous work and for the observed H₂/2H loss mechanisms detailed previously [26], we cannot distinguish between H₂ and 2H losses in our mass spectra [27]. For the 6.5 mJ/pulse train, losses of two, three, and four C₂(H₂) units are observed, furthermore, all of which are followed by dehydrogenation to give a pure carbon cluster.

The most striking aspect of the fragmentation pattern observed in isoviolanthrene is how early the formation of smaller carbon clusters takes place. C₇⁺ is formed after two laser pulses using 4.0 mJ/pulse and C_n⁺ (*n* = 11–15) are all observed to form after one laser pulse with 6.5 mJ/pulse. In contrast to the dibenzopyrenes, C₇⁺ and C₁₈⁺ are both formed in the fragmentation of isoviolanthrene and even very faint C₂₀⁺ signals can be observed. At this point it is important to note that the signals pertaining to C₁₀⁺ (120 *m/z*) are at the cutoff of the stability region of the ion trap. We refrain from drawing any conclusions about these masses.

In the case of dicoronylene fragmentation (Fig. 3), a direct comparison with the fragmentation patterns of the dibenzopyrene isomers presents more distinctive differences compared to isoviolanthrene and the dibenzopyrenes. In dicoronylene, H₂ loss appears to dominate in the competition between H₂ loss and the losses of C₂(H₂) units, but it is worth mentioning that as the laser pulse energy and numbers of laser pulses are increased, a greater amount of individual H-losses are observed after the first 4–5 pairs of H₂/2H are lost. It is only after a majority of parent ions is dehydrogenated in the trap (after 4 laser pulses) that carbon clusters between C_n, *n* = 32, 34, 36, 38, 40, 42, 44, 46, *i.e.*, clusters formed by sequential or concurrent C₂ losses from C₄₈⁺, are formed. This is in line with previous observations that larger PAHs tend to dehydrogenate prior to losing carbon atoms from its carbon skeleton [22,23].

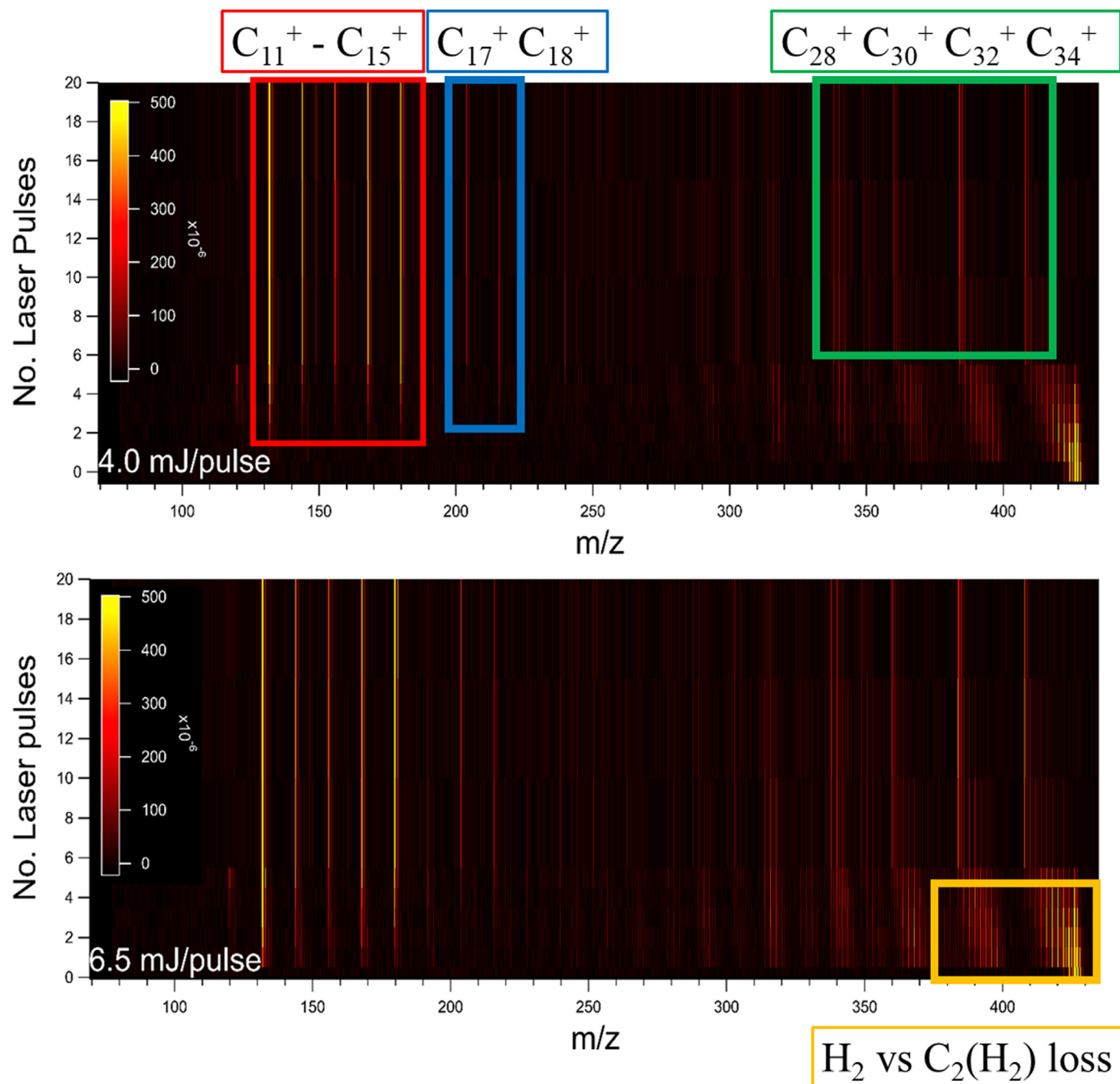


Fig. 2. Two-dimensional TOF-MS representation of the laser-induced photofragmentation of the isoviolanthrene cation. In the upper panel for 4.0 mJ/pulse and in the lower panel for 6.5 mJ/pulse. Each panel shows the number of laser pulses on the y-axis, the m/z ratio on the x-axis and the color scale indicates the strength of the mass peaks in arbitrary units. In the upper panel, the $C_{11}^+ - C_{15}^+$ clusters are highlighted in red, the $C_{17}^+ - C_{18}^+$ clusters are highlighted in blue, and the $C_{28}^+ - C_{34}^+$ clusters are highlighted in green to guide the eye. In the lower panel, the region where H_2 and $C_2(H_2)$ losses are observed in competition, is highlighted in orange.

Similar to isoviolanthrene, the fragmentation of dicoronylene also reveals an early formation of smaller carbon clusters (C_n^+ , $n = 11 - 15$). In both the 4.0 and 6.5 mJ/pulse matrices in Fig. 3, the formation of these carbon clusters is observed clearly after 3 and 1 laser pulses, respectively. Thus, the formation of these smaller carbon clusters appears to still be in direct competition with C_2 losses from the dehydrogenated C_{48}^+ cluster, and to a certain extent with the dehydrogenation of the parent species as well. This implies that there are considerable competing photoactivated dynamical effects within the molecule, involving geometric rearrangements that could facilitate losses of the aforementioned

smaller carbon clusters. These observations are in line with our prior work where the formation of a pure carbon cluster was preceded by the cluster retaining a few H atoms in its formation [24]. This aspect of the carbon cluster formation, *i.e.*, the retention of H atoms, is discussed in detail in section 3.5.

Equally noticeable as the clear formation of $C_{11}^+ - C_{21}^+$ species is the near complete absence of C_n^+ species in the range $n = 22 - 31$. Prior studies on the size-dependent stability of carbon clusters employing ion mobility techniques [28,29] showed two possible geometries of the carbon clusters; both monocyclic and bicyclic geometries whose structural properties have been previously

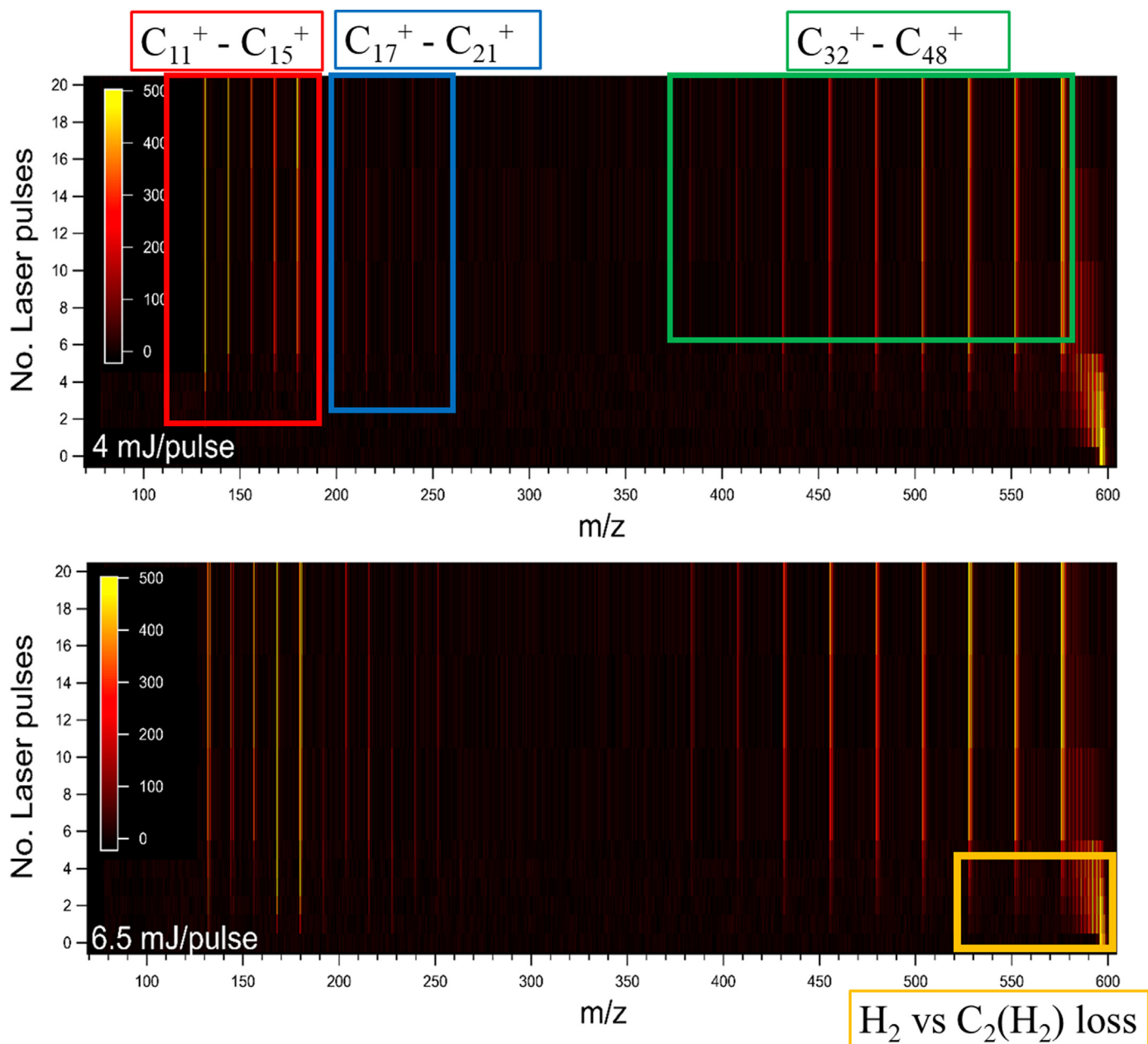


Fig. 3. Two-dimensional TOF-MS representation of the 4 mJ/pulse (top) and 6.5 mJ/pulse (bottom) laser-induced photofragmentation of the dicoronylene cation. Similarly, as in Fig. 2, the C_{11}^+ – C_{15}^+ clusters are highlighted in red, the C_{17}^+ – C_{21}^+ clusters are highlighted in blue, and the C_{32}^+ – C_{48}^+ clusters are highlighted in green. In the lower panel, the region where H_2 and $C_2(H_2)$ competitive losses are observed, is highlighted in orange.

investigated [30]. The most stable planar bicyclic structures comprise two rings which can range from ten up to fifteen carbon atoms each and are connected via one, two, or four covalent C–C bonds [31].

There are some conclusions that can be drawn from the almost complete lack of carbon clusters in this intermediate size range. First, is that stable fullerene structures are expected down to C_{32}^+ [29,32] and the crossover to fullerene stability occurs between C_{20} and C_{30} [33]. The lack of structures below C_{32}^+ hints that the larger carbon clusters formed in this top-down fragmentation route from PAHs, are indeed in the form of cages where C_{32}^+ constitutes the last possible fullerene that can be formed by subsequent C_2 losses as has been observed in the fragmentation of larger PAHs [23,34]. Second is that bicyclic (or C_n^+ , $n = 22$ – 31 , to be exact) structures are not

viable products in this top-down formation of PAHs in comparison to fullerenes (C_n^+ , $n \geq 32$) and cyclo[n]carbons (C_n^+ , $n = 10$ – 21) that appear to be stable fragmentation products of PAHs (see discussion below).

3.2. Quantizing the energies of H-losses

As our results imply the importance of carbon cluster formation it is relevant to explore the extent of quantitative information we can retrieve from our experiment regarding the swift H-losses from the PAH cations to gain insight into supposed energetics of the carbon cluster formation.

H cleavages from various sites on PAHs have been studied by experiments accompanied by DFT calculations [15]. It is found that

H binding energies are independent of molecule size and the degree of dehydrogenation, but there are slight dependencies on the edge structure. The binding energy of the first H atom is of the order of 5 eV but the binding energy of the second is around 4 eV. In cases of trios or quartet H-edges the binding energies can vary from 3.8 eV to 4.9 eV. Summing together the four solo and eight duo H atoms in dicoronylene, this equates to 88 eV while for two solo, four duos and two quartos this equals 79.4 eV for isoviolanthrene.

Some insight can be drawn from this information particularly when compared to available absorption cross sections of PAH cations [35] which include dicoronylene but not isoviolanthrene. The closest PAH in size to isoviolanthrene that is included is ovalene ($C_{32}H_{14}$) which we can roughly use as a proxy for isoviolanthrene ($C_{34}H_{18}$).

The computed cross section of the dicoronylene cation has a peak right around 2 eV (620 nm) equal to 100 Mb, while that for ovalene does not have such a large cross section at 2 eV, but a smaller bump just above 2 eV that equals 50 Mb approximately. For the time being, we will assume a cross section of 50 Mb at 2 eV for isoviolanthrene. If each laser pulse contains 40 or 65 mJ/cm²/pulse, then in the case of dicoronylene ($\sigma = 1 \times 10^{-16}$ cm²/molecule) a single laser pulse is capable of dispensing at maximum 4 or 6.5×10^{-18} J (25 or 40 eV) per molecule. This means that to overcome the 88 eV of energy required to remove all the H atoms from dicoronylene, the molecules would require 3–4 pulses at 4 mJ/pulse and 2–3 pulses at 6.5 mJ/pulse.

Comparing these numbers to Fig. 3, it appears that the C_{48}^+ (dehydrogenated parent signal) starts growing in around 2–3 pulses in the 4 mJ/pulse experiment and at 2 pulses in the 6.5 mJ/pulse experiment. This can also be roughly seen by the C_{48}^+ traces in the two experiments shown in Fig. 4 below.

In the case of isoviolanthrene, slightly less energy would be required for complete dehydrogenation (79.4 eV), but the cross section we can expect to be approximately 2x smaller if we use that of ovalene as a proxy ($\sigma = 5 \times 10^{-17}$ cm²/molecule). This leads to a

single laser dispensing 12.5 or 20 eV per molecule which requires 6 pulses in the 4 mJ/pulse experiment and 4 pulses in the 6.5 mJ/pulse experiment. By inspecting Fig. 3 we see the dehydrogenated parent appear around 5 pulses. Since we are estimating the cross section of isoviolanthrene, these numbers should be taken as rough estimates, though overall they appear to match reasonably with our experimental values.

There are many factors that can impact these estimates including how the cross sections change with the removal of H atoms which are unaccounted for [36]. There could still be significant energy left over that could vibrationally excite the molecules or even rupture the aromatic C–C bonds in the PAH cation skeletons. On the surface this could indicate that a reasonably small energy that is left over the photon absorption is required to form the smaller carbon clusters as will be discussed below, hinting at C–C aromatic bond ruptures taking place concurrently to C–H losses.

3.3. Competition between small and big carbon cluster formation

Fig. 4 displays the integrated peak areas of the pure carbon clusters formed in the laser-induced dissociation of both isoviolanthrene and dicoronylene. The peak areas have been normalized in the same manner as described in our previous work [24].

In the case of isoviolanthrene (Fig. 4a & b), it is apparent that using 4.0 mJ/pulse preferentially gives rise to smaller carbon clusters (C_n^+ , $n = 11–15$), rather than larger ones (C_n^+ , $n = 24, 26, 28, 30, 32, 34$). In fact, for the large clusters only significant C_{32}^+ and C_{34}^+ signals have been found. Using 6.5 mJ/pulse does not appear to change this fragmentation pattern significantly. C_{11}^+ is the most prevalent fragment that appears and is followed by C_{15}^+ , C_{14}^+ , and C_{12}^+ . The biggest change between the 4.0 and 6.5 mJ/pulse measurements is the initial rise in the yield of C_{11}^+ (and to a lesser extent, C_n^+ , $n = 12, 14, 15$) is steeper in the 6.5 mJ/pulse experiment.

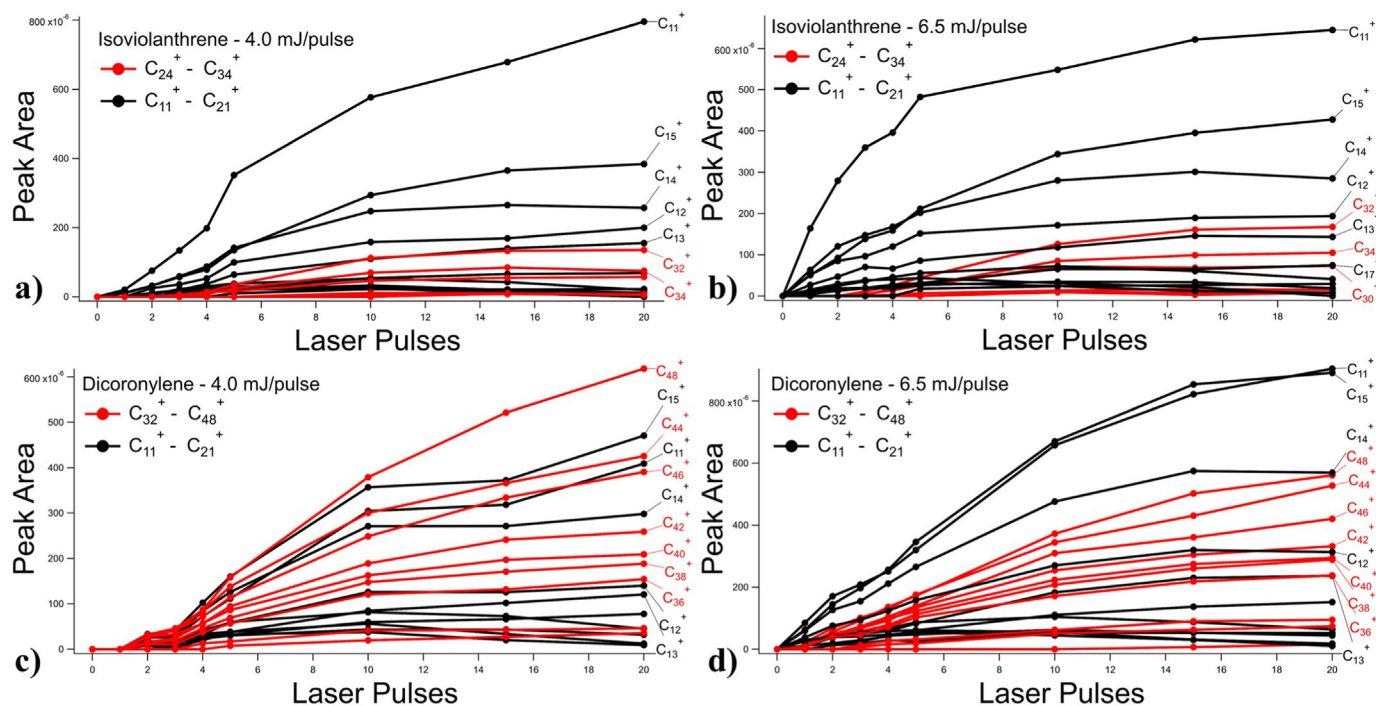


Fig. 4. Normalized peak areas of the carbon clusters formed in the dissociation of Isovianthrene, a) & b), and Dicoronylene, c) & d). Smaller carbon clusters (C_n^+ , $n = 11–21$) are depicted in black and larger carbon clusters (C_n^+ , $n \geq 24$) in red. The traces for the largest observed masses are labelled.

For dicoronylene (Fig. 4c & d), there is a more tangible competition between the formation of larger (C_n^+ , $n \geq 32$) and smaller (C_n^+ , $n = 10-21$) carbon clusters in the 4.0 mJ/pulse measurements. Therein, the largest mass peak observed is C_{48}^+ which corresponds to the fully dehydrogenated carbon skeleton of dicoronylene. The next stronger mass signals are found for C_{15}^+ , C_{44}^+ , C_{11}^+ , C_{46}^+ and C_{14}^+ , followed by C_n^+ ($n = 36, 38, 40, 42$), evidencing a clear competition in the formation of smaller and larger carbon clusters.

When the laser energy is increased to 6.5 mJ/pulse to induce dissociation of dicoronylene, the fragmentation pattern starts to resemble more what is observed in isoviolanthrene. C_{11}^+ and C_{15}^+ are now the strongest mass peaks, followed by C_{14}^+ and C_n^+ ($n = 42, 44, 46, 48$). This is in line with what is observed for isoviolanthrene where C_n^+ ($n = 11, 14, 15$) are the most dominant mass signals while larger carbon clusters are on par with the likes of C_{12}^+ and C_{13}^+ .

It is also interesting to investigate how the total energy, *i.e.*, the energy per pulse times the number of pulses, affects the dissociation behavior. For this, mass spectra recorded with 4.0 mJ/pulse and 6.5 mJ/pulse for different numbers of pulse trains, can be compared to search for dynamical differences in the competition between the small and large cluster fragmentation of the two PAH cations. However, direct comparisons even when looking at differences between these two regimes, is difficult due to the many effects that need to be disentangled for them to provide further insights into the underlying fragmentation mechanics. As the discussion wrought from these comparisons can only provide tentative insights at the current time, they are presented in the SI.

3.4. Branching ratios of smaller carbon clusters

The branching ratios of the C_n^+ ($n = 11-18$) carbon clusters are presented in Fig. 5. Larger carbon clusters up to C_{21}^+ were observed as well in the mass spectra, but as stated before, at a much lower abundance; their extracted branching ratios were around 1% with large, propagated errors and are not shown. The branching ratios are calculated by dividing the peak area of a corresponding fragment with the combined peak areas of all the carbon cluster peaks in this analysis, *i.e.*,

$$BR_{C_n^+} = \frac{A_{C_n^+}}{\sum_{n=11}^{18} A_{C_n^+}}$$

There are some interesting trends to be noted in the experimentally derived branching ratios of the C_n^+ ($n = 11-18$) carbon clusters formed from isoviolanthrene and dicoronylene for different numbers of pulses (*i.e.*, total energy). First, in many cases the branching ratios are remarkably similar. *E.g.*, the branching ratios of C_{14}^+ do not appear to deviate much from 15 to 20% for both PAHs at 4.0 and 6.5 mJ/pulse. A similar trend is observed for C_{15}^+ where the average for isoviolanthrene is between 15 and 20% and for dicoronylene between 20 and 25%. For more than 5 laser pulses, the same can be said for C_{17}^+ where the branching ratios reach a plateau around 4% in all experiments for both PAHs.

Second, the branching ratios of C_{12}^+ and C_{13}^+ are remarkably similar in all instances apart from the 4.0 mJ/pulse measurement of dicoronylene. In that specific measurement the average branching ratio is relatively stable at 5%, but at a higher value of 10% in the other experiments.

C_{16}^+ and C_{18}^+ are only observed for a select number of laser pulses. C_{16}^+ grows in immediately from both PAHs but starts depleting already at 3 laser pulses and is almost entirely absent at 20 pulses. The mass peak becomes so small that the error from the fit used to integrate the peak, becomes larger than the error of the branching ratio. For C_{18}^+ , an average branching ratio of 4% from isoviolanthrene

and 6% from dicoronylene is obtained at 4 laser pulses. However, with increasing the number of laser pulses, the branching ratio reduces until the species is effectively depleted at 20 pulses. For both C_{16}^+ and C_{18}^+ , we observe their formation, but they appear to be less favored products as the fragmentation process is driven forward.

The case for C_{11}^+ shows the largest distribution of branching ratios between the laser pulse energies and the two PAHs. For isoviolanthrene, C_{11}^+ is the most abundant fragment in all the experiments with the branching ratio averaging between 40 and 45%. For dicoronylene, there is a larger divide in the branching ratios between the 4.0 and 6.5 mJ/pulse experiments. For 4.0 mJ/pulse the branching ratio averages out around 10% but around 25% for 6.5 mJ/pulse. The smaller yield of C_{11}^+ in the dicoronylene experiments translates to a larger yield in larger cluster species, *i.e.*, C_n^+ ($n = 14-18$).

Many similarities arise when these fragmentation patterns are compared with those of the dibenzopyrenes studied previously [24]. Therein, a remarkable similarity was observed in the branching ratios of the C_n^+ ($n = 11-15$) species which appears to be mimicked here by isoviolanthrene and dicoronylene to a certain extent. The branching ratios of C_{12}^+ and C_{13}^+ both plateaued around 10%, which is what is observed here apart from the lower laser power experiment of dicoronylene. The largest spread in the branching ratios was found in C_{11}^+ (30–60%) which is likewise what we observe here (10–40%). Finally, the C_{14}^+ and C_{15}^+ branching ratios, like the C_{12}^+ and C_{13}^+ ones, averaged out to a similar ratio observed here, *i.e.*, 15–20%.

3.5. Formation of smaller carbon clusters

In the work by West *et al.* [37], they identified a formation route to the pure C_{14}^+ carbon cluster from pyrene. Before its formation, the cluster retained 1–3 H atoms, which were subsequently eliminated. It was hypothesized that the remaining carbon cluster formed an ionized cyclo[14]carbon molecule. Concerning isoviolanthrene and dicoronylene, the observed mass peaks corresponding to $C_nH_x^+$ ($n = 11-15$; $x = 1-3$) tell two different stories that appear indicative of the size-dependency of PAH photofragmentation behavior.

Figs. 6 and 7 show $C_nH_x^+$ ($n = 11-15$; $x = 1-3$) mass peaks from the fragmentation of isoviolanthrene and dicoronylene, respectively. The left vertical panel shows the peak area of C_nH^+ mass signals (solid lines) and the C_n^+ mass signals multiplied by a factor, *A*, to account for the expected ^{13}C contribution of the preceding mass. The factor *A* changes with the mass of the carbon cluster and is calculated from their natural abundances: $A = 0.119, 0.130, 0.141, 0.151, 0.162$ for C_n^+ , $n = 11, 12, 13, 14, 15$, respectively. If the solid lines are above the broken lines, this indicates measurable $C_nH_x^+$ mass signals seeing that they equate to the amount of C_nH_x in the mass peak in surplus of the ^{13}C contribution of the preceding mass peak. In Fig. 6 these trends are then continued in the middle vertical panel for $C_nH_2^+$ vs C_nH^+ signals, and the right vertical panel for $C_nH_3^+$ vs $C_nH_2^+$ signals. In some cases, there were no observable $C_nH_3^+$ peaks in the mass spectrum in the 4.0 mJ/pulse experiment, which is why those traces are missing.

In the case of isoviolanthrene, there are clear indications of $C_nH_x^+$ fragments being formed along with the pure carbon clusters. When the C_nH^+ mass signals are compared with the ^{13}C component expected from the C_n^+ signals, the C_nH^+ yield is almost always higher than what is expected from the ^{13}C component (see Fig. 6, left panels). In the case of $C_{11}H^+$, its yield is largest after 1–5 laser pulses, but then drops down to the expected ^{13}C level. A similar depletion in the mass signal is observed for $C_{12}H^+$ while $C_{13}H^+$, $C_{14}H^+$ and $C_{15}H^+$ appear to be continually replenished in the fragmentation with their mass signatures constantly above the ^{13}C level.

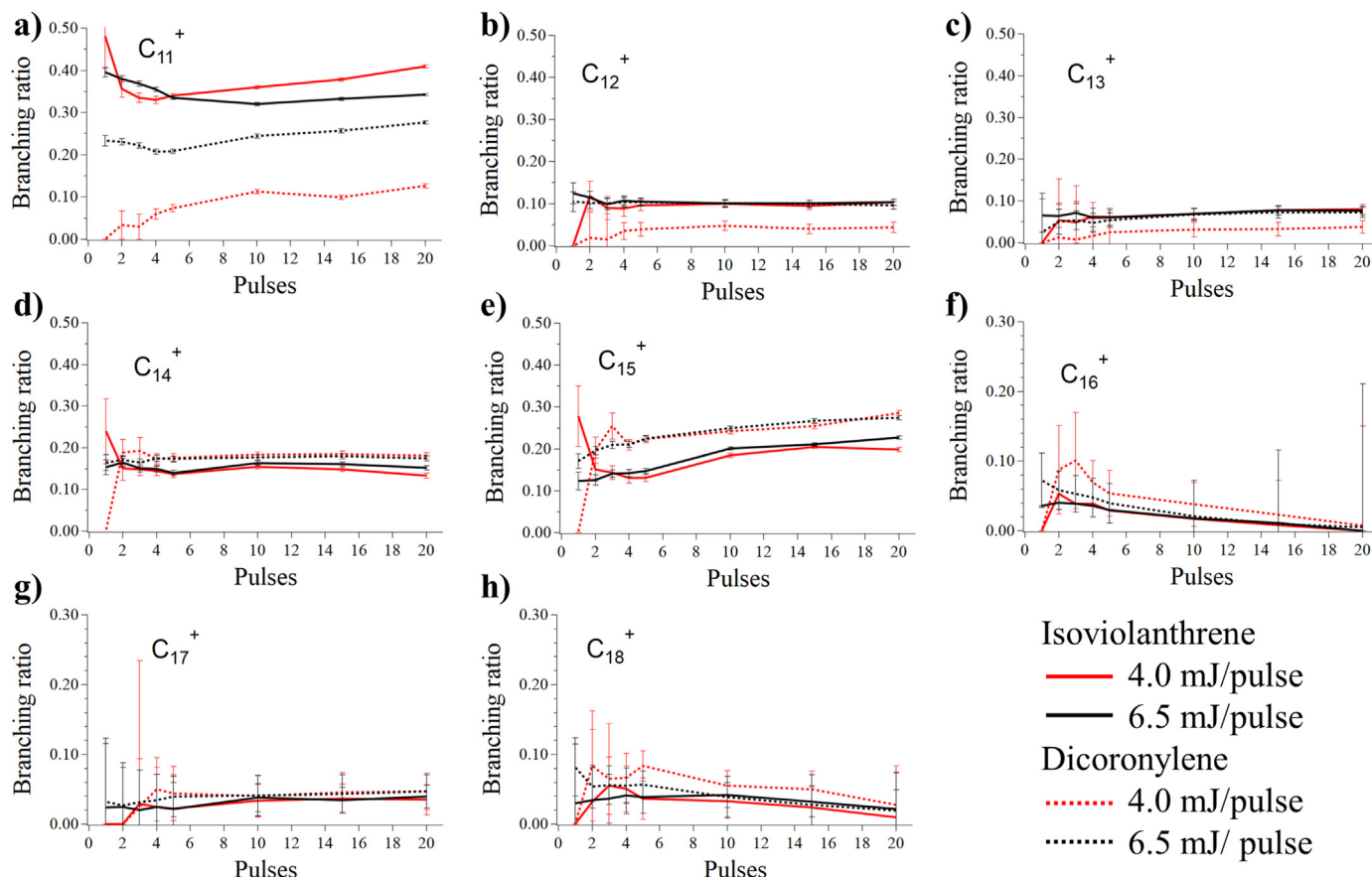


Fig. 5. Branching ratios of the C_n^+ ($n = 11-18$) carbon clusters (panels a to h) observed in the laser-induced fragmentation of both isoviolanthrene and dicoronylene. Note that the y-axis is scaled to 0.50 in panels a) through e) but scaled to 0.30 in panels f) through h) such that the branching ratio trends are more apparent.

There are also clear indications that poly-acetylene $C_nH_2^+$ isomers are initially formed along with the carbon clusters (Fig. 6, middle columns). Particularly in the case of the 6.5 mJ/pulse experiments, the $C_nH_2^+$ yields are significantly higher than what is expected from the ^{13}C component of C_nH^+ (we assume negligible contributions from $C_{n-2}C_2$) for 1–5 laser pulses. After 5 laser pulses, the signals reach or appear to fall below the plateau of the ^{13}C contributions, where in most cases, the mass peaks are not intense enough to be detected confidently or separated from the baseline.

$C_nH_3^+$ signals are also observed in the fragmentation of isoviolanthrene but only in the 6.5 mJ/pulse experiments, except for $C_{11}H_3^+$ (Fig. 6, right panels). The observed $C_nH_3^+$ mass signals appear short-lived. They appear reasonably stronger than the ^{13}C component of $C_nH_2^+$ at one or two laser pulses and are then subsequently depleted rather quickly. The case of $C_{11}H_3^+$ appears to be an extreme case where $C_{11}H_3^+$ signals are observed even at 10 laser pulses and above. This might go hand-in-hand with the fact that C_{11}^+ is the most common carbon cluster photoproduct of isoviolanthrene (as well as the dibenzopyrenes) and indicates that there are more fragmentation pathways energetically available that eventually form C_{11}^+ (via the retention of three H atoms).

Curiously, dicoronylene appears not to favor the same mechanism for the formation of carbon clusters as isoviolanthrene (see Fig. 7). When the C_nH^+ signals are compared with the $C_{n-1}^{13}C^+$ signals (left panel), there is only slight evidence of C_nH^+ signals for $n = 12, 13$. C_nH^+ , $n = 11, 14, 15$ signals are below or on par with the expected ^{13}C signals from the carbon cluster. Even for the $C_nH_2^+$ signals, there is mostly tentative evidence apart from the $C_{11}H_2^+$ and $C_{12}H_2^+$ where the signals are stronger than the expected ^{13}C signal

below and above 5 laser pulses, respectively. Considering that dicoronylene appears to initially favor H-losses, the lack of C_nH^+ signals is reasonable. If the formation of smaller carbon rings stems from a mostly dehydrogenated parent, it makes sense that the nascent carbon clusters are less likely to retain H atoms.

4. Discussion

4.1. Comparisons with previous work

In this section we will detail what chemical intuitions of the observed PAH fragmentations can be gained in comparison with previous works. In our previous work [24], we found that the structural isomers dibenzo[a,e]pyrene, dibenzo[a,h]pyrene and dibenzo[a,l]pyrene produced C_n^+ ($n = 11-15$) carbon clusters in very similar branching ratios upon irradiation. The principal results of this prior work implied that despite different symmetries of the parent PAH cations, the fragmentation pathways appear to be very similar. As a follow up in the present work, it is interesting to discuss how the fragmentation of isoviolanthrene and dicoronylene compares with that of the dibenzopyrene isomers which allows to explore how the size of a parent PAH cation may affect fragmentation pathways.

The fragmentation patterns of isoviolanthrene (Fig. 2) imply that there is an initial competition not only between $H_2(/2H)$ -losses and C_2H_x ($x = 1-2$) losses, but also C–C aromatic bond ruptures that eventually lead to $C_nH_x^+$ ($n = 11-15$, $x = 1-3$) clusters separating from the parent. The competition between $H_2(/2H)$ - and C_2H_x loss is observed as a series of $C_{32}H_x^+$ ($x = 0-14$; 384–398 amu), $C_{30}H_x^+$

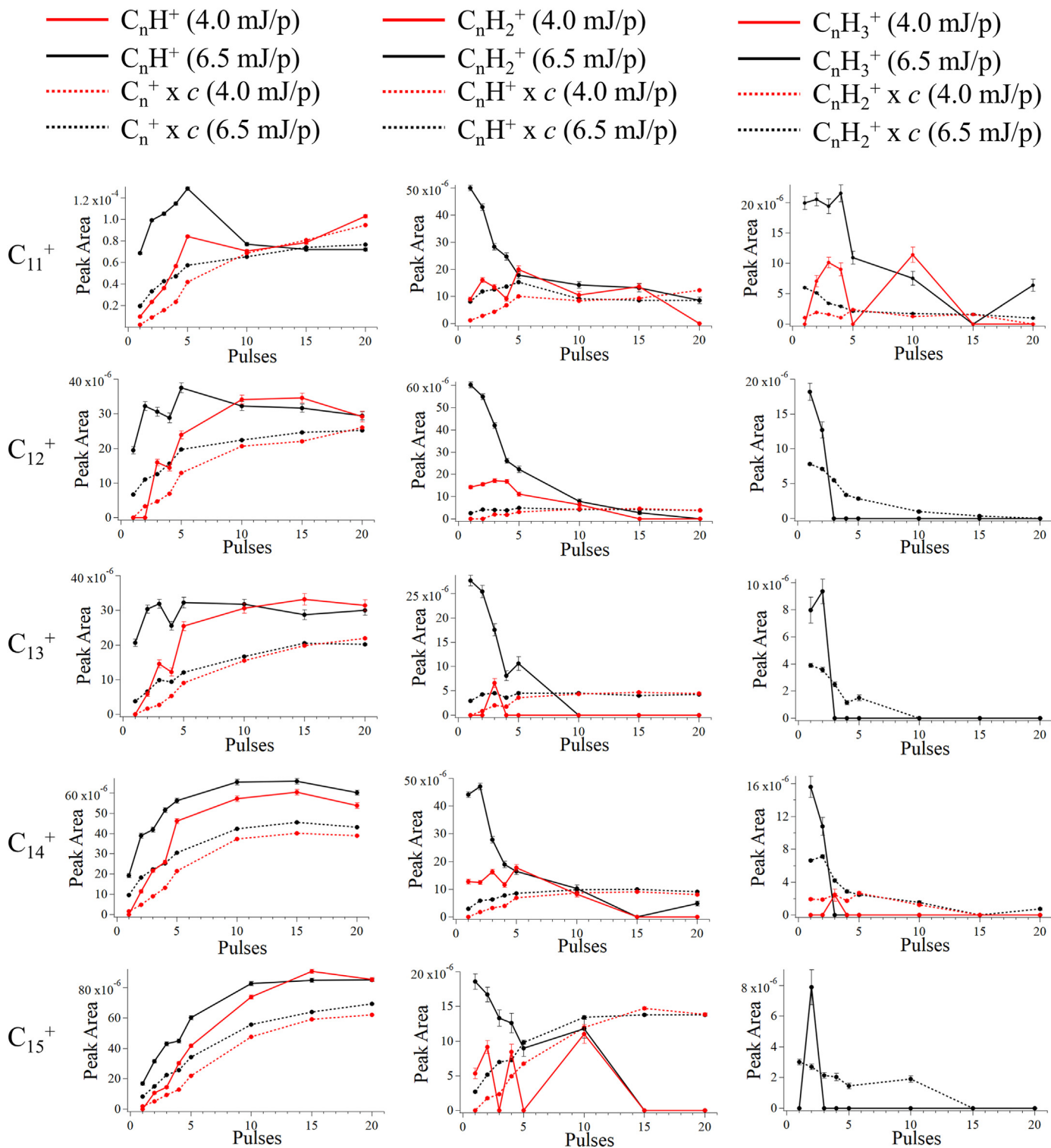


Fig. 6. $C_n H_x^+$ ($n = 11-15$; $x = 1-3$) mass peaks from the fragmentation of isoviolanthrene.

($x = 0-12$; 360–372 amu), $C_{28}H_x^+$ ($x = 0-10$; 336–346 amu), and $C_{26}H_x^+$ ($x = 0-8$; 312–320 amu) mass signatures that can only be formed if the parent loses one, two, three or four C_2H_2 moieties, respectively, from its carbon skeleton. This is similar to what was observed in the fragmentation of the dibenzopyrene isomers. However, whereas the dibenzopyrenes also exhibited CH losses from the parent structure, we only observe CH losses in the case of

isoviolanthrene after an initial two C_2H_x moieties are lost, so from $C_{30}H_x^+$ downwards in mass. These appear as $C_{29}H_x^+$ ($x = 3, 5, 7$; 351, 353, 355 amu) mass signals. This is curious because it could point to a loss of an allylic species (C_3H_x) after an initial C_2H_2 unit is lost which could be an indicator of the formation of the pentalene unit, similar to what has been observed from the C_2H_2 loss from naphthalene [14].

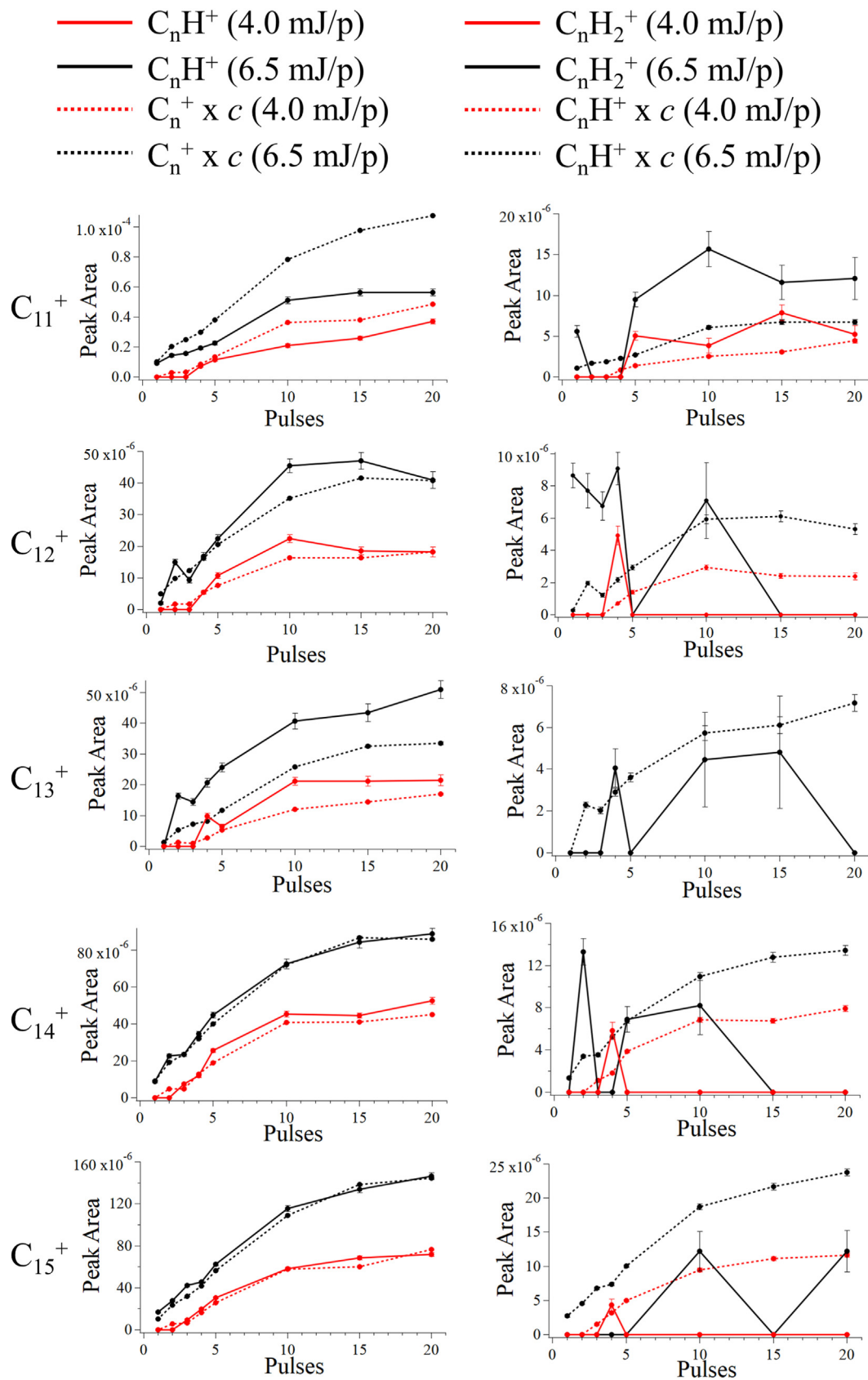


Fig. 7. $C_nH_x^+$ ($n = 11-15$; $x = 1-3$) mass peaks from the fragmentation for dicoronylene. No or negligible $C_nH_3^+$ mass peaks were observed in the fragmentation mass spectra of dicoronylene.

Meanwhile, the fragmentation patterns of dicoronylene (Fig. 3) show that the initial dominating fragmentation mechanism is that of $H_2/2H$ -losses along with the apparently facile formation of C_7^+ prior to C_2 -losses from the carbon skeleton of the parent. This could make sense in a statistical fragmentation paradigm where the absorbed photon energy is equally distributed over the molecule [38,39]. In this paradigm, the chemical bonds in the molecule with comparable energies are broken seemingly at random, and with the large amounts of C atoms compared with H atoms, there are statistically more options that lead to H-losses than C_2 -losses as H-loss only requires one bond to break and $C_2(H_2)$ -loss requires breaking at least two preselected bonds in the case of dicoronylene.

The way that the smaller carbon clusters (C_n^+ , $n = 11-15$) are formed (see section 3.5) also reflects the fact that larger more compact PAHs like dicoronylene initially prefer dehydrogenation as a fragmentation process. This preference is reflected in formation of the smaller carbon clusters. With most H atoms already lost from the carbon skeleton, the chances of the smaller carbon clusters breaking off the PAH skeleton with a few H atoms, become smaller. Thus, with most of the energy initially spent on cleaving the C–H bonds in dicoronylene, the smaller carbon clusters need to be broken by sequential or concurrent C_2 losses, or the skeleton breaking apart forming a smaller C_n^+ ($n = 11-21$) carbon cluster. However, for smaller and less compact PAH skeletons, like isoviolanthrene, there is already a competition between the C–H bond cleavages and the $C_2(H_2)$ losses and C–C aromatic bond ruptures. This is manifested by the smaller carbon clusters initially breaking off the PAH skeleton which has not lost all or most of its H atoms.

The competition between C_2 -loss and aromatic C–C ruptures in the PAH skeleton appears to thus be verified in the case of dicoronylene by the early onset of the C_7^+ mass peaks when compared to complete dehydrogenation to form C_{48}^+ (both formed after 2 pulses of 4 mJ/pulse, Fig. 3). This competition is visualized by employing chemical intuition based on existing literature works [14,17,34,40–44] in the SI.

Not many studies exist that have investigated the wavelength dependent fragmentation of PAHs to reveal small carbon clusters. Using 480 nm wavelength light from an OPO and a Xe arc lamp, Joblin [18] found C_7^+ to be a dominant product in the fragmentation of coronene while Zhen *et al.* found $C_{16}^+ - C_{21}^+$ carbon clusters forming from the laser-induced fragmentation of the HBC cation using 532 nm [23], but it is worth noting that their experiment was not optimized for smaller carbon clusters. Combined with our previous study on the dibenzopyrenes (using 620 nm laser light), earlier results from the literature appear to indicate a certain wavelength sensitivity of the ionized carbon cluster product yields. This is further discussed below.

4.2. Astrophysical implications

While the work presented here applies to PAH cations as we are experimentally limited to trapping charged species, the processes hereto forth discussed are transferable to interstellar processes as both neutral and charged PAHs, both expected to be present in the interstellar medium, are predicted to dissociate similarly [3,12]. It is expected that energetic processing of the two PAHs presented in this work using 620 nm light will trigger dissociation channels that generally also apply in space, albeit involving different excitation mechanisms. The fragmentation of PAHs of various sizes and shapes has been studied in different wavelength ranges. In the optical range, the first fragmentation steps of dicoronylene have been studied by Joblin [18] who found that photodissociation proceeds until full dehydrogenation has been achieved prior to sequential C_2 losses.

The use of optical frequencies is useful to investigate the variety

of potential fragmentation products of PAHs [22–24]. Performing such an experiment in the VUV region comes with some practical problems, mainly owing to the propensity of PAHs to doubly ionize rather than fragment upon absorption of VUV photons [45,46]. However, as described above, using optical frequencies can allow us to impart 25–40 eV worth of energy onto a single molecule in a single laser pulse, roughly the equivalent of 2–4 UV photons in space.

This photofragmentation behavior of PAHs is also dependent on the radiation field. This particularly applies to high-energy regions such as Active Galactic Nuclei (AGN) where photochemistry is driven by 0.2–10 keV photons produced by gas accretion onto a supermassive black hole. As X-ray absorption of PAHs leads to a variety of other ionized products [47,48], including some of the smaller carbon clusters we observe in this work.

In the case of interstellar shocks, the dominating PAH-damaging mechanism at shock velocities below 75 km/s is impact by He or H. Depending on the gas column density and PAH size, each individual PAH will typically collide with one or two He atoms with enough energy to remove a carbon atom before being injected into the ISM [49]. At higher velocities (above 100 km/s), collisions with electrons also contribute to damaging PAHs, but this effect gets smaller with increasing PAH size, making atom knockout by collisions with He and H, dominating with the largest interstellar PAH molecules. While collisions of PAHs with highly charged ions mostly form multiply charged PAHs which can subsequently undergo coulomb explosions [50], collisions of small PAHs with energetic He^{2+} ions have revealed a host of positively charged hydrocarbons [51].

This work shows that PAHs of different sizes and symmetry favor similar fragmentation pathways and more importantly, products. When it comes to considering, e.g., potential molecular carriers of the diffuse interstellar bands, intuitively one would search for products of abundant interstellar molecules (like PAHs), that display some general characteristics of photo-resistivity to fragmentation. Here, we argue that the ionized carbon clusters we observe in this work should be considered viable candidates as they are all common products in the fragmentation of various PAHs, i.e., abundances may be higher than initially expected.

Furthermore, as both PAHs [9] and other molecules like HC_3N [52] are now starting to be used to extract information about high-redshift galaxies and support identification of AGN and even tidal disruption events [53,54], searching for these ionized carbon clusters in extra-galactic regions would be a worthwhile endeavor, particularly in regions which have been heavily energetically processed.

4.3. Carbon clusters and cyclo[n]carbons

Of particular interest in this discussion is the structure of the carbon clusters we observe to form from the irradiation of the PAHs studied here and in our previous work [24]. So-called magic number carbon clusters have been observed to form in laser ablation experiments since the 1980's [55] and much work has been devoted to linear carbon clusters (e.g. see Refs. [56–60] and references therein) seeing that linear C_3 and C_5 have been known interstellar molecules since the late 1980's [61–64]. Indeed, the idea of carbon clusters forming carbon rings was first evidenced with photoelectron spectroscopy of anionic carbon clusters in the 10–29 atom size range [65], and this was further expanded to show that anionic carbon clusters of sizes $C_{10} - C_{18}$ show an affinity for monocyclic structures. However, neutral C_{20} , C_{24} , and C_{28} all show an affinity for bicyclic structures [30] as well as monocyclic structures [28,29]. The fragmentation of both of these larger monocyclic and bicyclic species split and form two smaller (closed-shell) monocyclic clusters such as C_{10} , C_{14} , etc. [66,67].

The presence of cyclic C_n carbon clusters has furthermore been detected in various experiments [68–75], and the closed-shell, doubly aromatic cyclo[n]carbons ($n = 10, 14, 18$) have been of particular interest because of their structural properties [76]. It has been theoretically shown that for C_n carbon clusters in the size range $n = 10–30$, the most stable structures are predicted to be cyclic C_{4m+2} clusters with $D_{(2m+1)h}$ symmetry and cumulenic bonding configurations, whereas cyclic C_{4m} clusters take the form of bond-alternating planar rings of $C_{(2m)h}$ symmetry (see Ref. [76] and references therein).

Recently, spectroscopic advances utilizing drift techniques and action spectroscopy have allowed the recording of the optical spectra of ionized cyclo[n]carbons van der Waals complexes with N_2 [77] and He [78]. The spectral signatures of these complexes show a distinct broadening for ionized doubly anti-aromatic cyclo[n]carbons ($n = 8, 12, 16$), but very sharp features for the ionized doubly aromatic ones ($n = 10, 14, 18$). Buntine *et al.* [77] discuss the possibilities of C_{14}^+ and C_{18}^+ potentially being carriers of one of the diffuse interstellar bands (DIBs), but because the second (weaker) sharp features in their spectra do not have any matches out of the known DIBs, such an assignment cannot be made at this time, particularly since the weakly attached N_2 molecule shifts the spectrum by an unknown amount.

The optical spectra recorded by Buntine *et al.* showed that the even numbered carbon clusters C_n^+ ($n = 12, 14$) display resonances in the 500–600 nm wavelength range, *i.e.*, below the wavelength used in our work to fragment the PAH cations. Meanwhile, larger carbon clusters, C_n^+ ($n = 16, 18, 20, 22, 24$), all absorb longer wavelengths than 620 nm. This could be a further indication that the C_n^+ ($n = 11–15$) carbon clusters observed in this work may not possess dissociative resonances that are accessible at 620 nm which would fit with the trend of optical spectra recorded by Buntine *et al.* Larger carbon clusters than C_{15}^+ , however, we observe sporadically before being depleted in the ion trap.

There is also recent work where the radiative cooling rates of C_n^+ ($n = 9, 11, 12, 17–27$) clusters have been measured being on the order of 10^4 s^{-1} [79]. These cooling rates appear to win out over unimolecular decay which contributes to the overall stability of these clusters as the fragmentation is quenched and cooling is primarily achieved through photon emission. This is an important point in terms of the duty cycle of our experiment where the laser repetition rate is 10 Hz and the pulse duration on the order of ns, there is a *ca.* 100 ms time frame for the photo-excited ionized cyclo[n]carbons to relax via photon emission rather than dissociate. We should note, however, that the laser power in our experiment is significantly higher than in the measurements of the radiative cooling rates so these comparisons must be made with care.

In the case of some ionized PAHs, like the perylene cation, there is more competition between radiative cooling and fragmentation [80] which could be why the carbon clusters presented in this work appear to easily survive in the ion trap during irradiation. However, for PAHs with hydroxy (-OH) groups attached, this radiative cooling is entirely missing [81]. These observations strongly hint at a photo-resistivity of ionized cyclo[n]carbons which could allow them to survive in the ISM for an even more extended time than PAHs.

5. Summary and conclusions

We have presented here the fragmentation patterns of two PAH cations, namely isoviolanthrene and dicoronylene as a continuation of our previous work detailing the fragmentations of three dibenzopyrene isomers [24]. The laser-induced fragmentations showcase complex but exceedingly similar pathways in the molecules which favor the formation of certain carbon clusters, in particular C_n^+

($n = 11–15$), which is also the case for dibenzopyrenes. Our work on the dibenzopyrenes showed that despite different starting symmetries, the fragmentation products were practically the same. In the present study we show that also for two geometrically very different PAHs, both in terms of geometry and size, the reaction products are still very similar.

The main take home message of this work is that it further supports a universal PAH fragmentation mechanism which would help understand and resolve the photochemistry of UV-rich interstellar regions such as photodissociation regions, but possibly also other environments in which PAHs are processed, *e.g.*, by electrons or cosmic rays. The exact fragmentation patterns involved are not known, but the mass spectra presented here hint for possible dissociation pathways. As with our previous work, this work emphasizes that C_n^+ ($n = 11–15$) carbon clusters are likely common fragment products from continued irradiation of PAHs. The present work also shows, in agreement with earlier work, the C_{32}^+ is the smallest stable cage species.

Author statement

H. R. Hrodmarsson: Data curation, formal analysis, investigation, writing – original draft, review & editing.

J. Bouwman: Methodology, formal analysis, investigation, writing, review & editing.

A. G. G. M. Tielens: Resources, investigation, review & editing.

H. Linnartz: Project administration, investigation, writing, review & editing.

Declaration of competing interest

The authors declare that they have no known competing financial interests or personal relationships that could have appeared to influence the work reported in this paper.

Data availability

Data will be made available on request.

Acknowledgments

H. R. H. acknowledges funding from the European Union's Horizon 2020 research and innovation programme under grant agreement No. 838372. J. B. acknowledges the Netherlands Organisation for Scientific Research (Nederlandse Organisatie voor Wetenschappelijk Onderzoek, NWO) for a Vidi grant (grant number 723.016.006) which supported this work. This work was supported in part by NASA's Solar System Exploration Research Virtual Institute (SSERVI): Institute for Modeling Plasma, Atmosphere, and Cosmic Dust (IMPACT).

Appendix A. Supplementary data

Supplementary data to this article can be found online at <https://doi.org/10.1016/j.ijms.2022.116996>.

References

- [1] A. Leger, J.L. Puget, Identification of the “unidentified” IR emission features of interstellar dust, *Astron. Astrophys.* 137 (1984) L5–L8.
- [2] L.J. Allamandola, A.G.G.M. Tielens, J.R. Barker, Polycyclic aromatic hydrocarbons and the unidentified infrared emission bands - auto exhaust along the Milky Way, *Astrophys. J.* 290 (1985) L25–L28, <https://doi.org/10.1086/184435>.
- [3] A.G.G.M. Tielens, Interstellar polycyclic aromatic hydrocarbon molecules, *Annu. Rev. Astron. Astrophys.* 46 (2008) 289–337, <https://doi.org/10.1146/annurev.astro.46.060407.145211>.

- [4] A.M. Burkhardt, K.L.K. Lee, P.B. Changala, C.N. Shingledecker, I.R. Cooke, R.A. Loomis, H. Wei, S.B. Charnley, E. Herbst, M.C. McCarthy, B.A. McGuire, with GOTHAM observations of TMC-1, *Astrophys. J. Lett.* 913 (2021) L18, <https://doi.org/10.3847/2041-8213/abfd3a>.
- [5] J. Cernicharo, M. Agúndez, C. Cabezas, B. Tercero, N. Marcelino, J.R. Pardo, P. de Vicente, Pure hydrocarbon cycles in TMC-1: discovery of ethynyl cyclopropenylidene, cyclopentadiene, and indene, *Astron. Astrophys.* 649 (2021) L15, <https://doi.org/10.1051/0004-6361/202141156>.
- [6] B.A. McGuire, R.A. Loomis, A.M. Burkhardt, K.L.K. Lee, C.N. Shingledecker, S.B. Charnley, I.R. Cooke, M.A. Cordiner, E. Herbst, S. Kalenskii, M.A. Siebert, E.R. Willis, C. Xue, A.J. Remijan, M.C. McCarthy, Detection of two interstellar polycyclic aromatic hydrocarbons via spectral matched filtering, *Science* 371 (2021) 1265–1269, <https://doi.org/10.1126/science.abb7535>.
- [7] L.J. Allamandola, G.G.M. Tielens, J.R. Barker, Interstellar polycyclic aromatic hydrocarbons - the infrared emission bands, the excitation/emission mechanism, and the astrophysical implications, *Astrophys. J. Suppl. Ser.* 71 (1989) 733–775, <https://doi.org/10.1086/191396>.
- [8] M. Frenklach, E.D. Feigelson, Formation of polycyclic aromatic hydrocarbons in circumstellar envelopes, *Astrophys. J.* 341 (1989) 372–384, <https://doi.org/10.1086/167501>.
- [9] I. García-Bernete, D. Rigopoulou, A. Alonso-Herrero, M. Pereira-Santaella, P.F. Roche, B. Kerkeni, Polycyclic aromatic hydrocarbons in seyfert and star-forming galaxies, *Mon. Not. Roy. Astron. Soc.* 509 (2021) 4256–4275, <https://doi.org/10.1093/mnras/stab3127>.
- [10] D. Rigopoulou, M. Barale, D.C. Clary, X. Shan, A. Alonso-Herrero, I. García-Bernete, L. Hunt, B. Kerkeni, M. Pereira-Santaella, P.F. Roche, The properties of polycyclic aromatic hydrocarbons in galaxies: constraints on PAH sizes, charge and radiation fields, *Mon. Not. Roy. Astron. Soc.* 504 (2021) 5287–5300, <https://doi.org/10.1093/mnras/stab959>.
- [11] I. Cherchneff, The Formation of Polycyclic Aromatic Hydrocarbons in Evolved Circumstellar Environments, *EAS Publications Series* 46 (2011) 177, <https://doi.org/10.1051/eas/1146019>.
- [12] A.G.G.M. Tielens, The molecular universe, *Rev. Mod. Phys.* 85 (2013) 1021–1081, <https://doi.org/10.1103/RevModPhys.85.1021>.
- [13] H. Andrews, C. Boersma, M.W. Werner, J. Livingston, L.J. Allamandola, A.G.G.M. Tielens, PAH emission at the bright locations of PDRs: the grandPAH hypothesis, *Astrophys. J.* 807 (2015) 99, <https://doi.org/10.1088/0004-637X/807/1/99>.
- [14] J. Bouwman, A.J. de Haas, J. Oomens, Spectroscopic evidence for the formation of pentalene⁺ in the dissociative ionization of naphthalene, *Chem. Commun.* 52 (2016) 2636–2638, <https://doi.org/10.1039/C5CC10090A>.
- [15] P. Castellanos, A. Candian, J. Zhen, H. Linnartz, A.G.G.M. Tielens, Photoinduced polycyclic aromatic hydrocarbon dehydrogenation: the competition between H- and H₂-loss, *Astron. Astrophys.* 616 (2018) A166, <https://doi.org/10.1051/0004-6361/201833220>.
- [16] S.P. Ekern, A.G. Marshall, J. Szczepanski, M. Vala, Photodissociation of gas-phase polycyclic aromatic hydrocarbon cations, *J. Phys. Chem.* 102 (1998) 3498–3504, <https://doi.org/10.1021/jp980488e>.
- [17] A.J. de Haas, J. Oomens, J. Bouwman, Facile pentagon formation in the dissociation of polyaromatics, *Phys. Chem. Chem. Phys.* 19 (2017) 2974–2980, <https://doi.org/10.1039/C6CP08349H>.
- [18] C. Joblin, Carbon Macromolecules in the Cycle of Interstellar Matter: Observational and Laboratory Experiments, in: *Semaine de l'Astrophysique Française, meeting held in Bordeaux, France, June 16-20, 2003*, *EdP-Sciences, Conference Series*, 175., 2003.
- [19] H.W. Jochims, H. Baumgartel, S. Leach, Structure-dependent photostability of polycyclic aromatic hydrocarbon cations: laboratory studies and astrophysical implications, *Astrophys. J.* 512 (1999) 500–510, <https://doi.org/10.1086/306752>.
- [20] C. Lifshitz, Energetics and dynamics through time-resolved measurements in mass spectrometry: aromatic hydrocarbons, polycyclic aromatic hydrocarbons and fullerenes, *Int. Rev. Phys. Chem.* 16 (1997) 113–139, <https://doi.org/10.1080/014423597230235>.
- [21] S.J. Pachuta, H.I. Kentamaa, T.M. Sack, R.L. Cerny, K.B. Tomer, M.L. Gross, R.R. Pachuta, R.Graham Cooks, Excitation and dissociation of isolated ions derived from polycyclic aromatic hydrocarbons, *J. Am. Chem. Soc.* 110 (1988) 657–665, <https://doi.org/10.1021/ja00211a001>.
- [22] J. Zhen, P. Castellanos, D.M. Paardekooper, H. Linnartz, A.G.G.M. Tielens, Laboratory Formation of fullerenes from PAHS: top-down interstellar chemistry, *Astrophys. J. Lett.* 797 (2014), <https://doi.org/10.1088/2041-8205/797/2/L30>.
- [23] J. Zhen, D.M. Paardekooper, A. Candian, H. Linnartz, A.G.G.M. Tielens, Quadrupole ion trap/time-of-flight photo-fragmentation spectrometry of the hexaperi-hexabenzocoronene (HBC) cation, *Chem. Phys. Lett.* 592 (2014) 211–216, <https://doi.org/10.1016/j.cplett.2013.12.005>.
- [24] H.R. Hrodmarsson, J. Bouwman, A.G.G.M. Tielens, H. Linnartz, Similarities and dissimilarities in the fragmentation of polycyclic aromatic hydrocarbon cations: a case study involving three dibenzopyrene isomers, *Int. J. Mass Spectrom.* 476 (2022), 116834, <https://doi.org/10.1016/j.ijms.2022.116834>.
- [25] V.M. Doroshenko, R.J. Cotter, Advanced stored waveform inverse Fourier transform technique for a matrix-assisted laser desorption/ionization quadrupole ion trap mass spectrometer, *Rapid Commun. Mass Spectrom.* 10 (1996) 65–73, [https://doi.org/10.1002/\(SICI\)1097-0231\(19960115\)10:1<65::AID-RCM447>3.0.CO;2-M](https://doi.org/10.1002/(SICI)1097-0231(19960115)10:1<65::AID-RCM447>3.0.CO;2-M).
- [26] S. Rodriguez Castillo, A. Simon, C. Joblin, Investigating the importance of edge-structure in the loss of H/H₂ of PAH cations: the case of dibenzopyrene isomers, *Int. J. Mass Spectrom.* 429 (2018) 189–197, <https://doi.org/10.1016/j.ijms.2017.09.013>.
- [27] B. West, S. Rodriguez Castillo, A. Sit, S. Mohamad, B. Lowe, C. Joblin, A. Bodi, P.M. Mayer, Unimolecular reaction energies for polycyclic aromatic hydrocarbon ions, *Phys. Chem. Chem. Phys.* 20 (2018) 7195–7205, <https://doi.org/10.1039/C7CP07369K>.
- [28] G. von Helden, M. Hsu, P.R. Kemper, M.T. Bowers, Structures of carbon cluster ions from 3 to 60 atoms: linear to rings to fullerenes, *J. Chem. Phys.* 95 (1991) 3835–3837, <https://doi.org/10.1063/1.460783>.
- [29] G. von Helden, M.T. Hsu, N. Gotts, M.T. Bowers, Carbon cluster cations with up to 84 atoms: structures, formation mechanism, and reactivity, *J. Phys. Chem.* 97 (1993) 8182–8192, <https://doi.org/10.1021/j100133a011>.
- [30] H. Handschuh, G. Ganteför, B. Kessler, P.S. Bechthold, W. Eberhardt, Stable configurations of carbon clusters: chains, rings, and fullerenes, *Phys. Rev. Lett.* 74 (1995) 1095–1098, <https://doi.org/10.1103/PhysRevLett.74.1095>.
- [31] G. von Helden, M.T. Hsu, N.G. Gotts, P.R. Kemper, M.T. Bowers, Do small fullerenes exist only on the computer? Experimental results on C₂₀^{+/−} and C₂₄^{+/−}, *Chem. Phys. Lett.* 204 (1993) 15–22, [https://doi.org/10.1016/0009-2614\(93\)85599-J](https://doi.org/10.1016/0009-2614(93)85599-J).
- [32] H. Kietzmann, R. Rochow, G. Ganteför, W. Eberhardt, K. Vietze, G. Seifert, P.W. Fowler, Electronic structure of small fullerenes: evidence for the high stability of C₃₂, *Phys. Rev. Lett.* 81 (1998) 5378–5381, <https://doi.org/10.1103/PhysRevLett.81.5378>.
- [33] P.R.C. Kent, M.D. Towler, R.J. Needs, G. Rajagopal, Carbon clusters near the crossover to fullerene stability, *Phys. Rev. B* 62 (2000) 15394–15397, <https://doi.org/10.1103/PhysRevB.62.15394>.
- [34] J. Zhen, P. Castellanos, D.M. Paardekooper, H. Linnartz, A.G.G.M. Tielens, Laboratory Formation of fullerenes from PAHS: top-down interstellar chemistry, *Astrophys. J. Lett.* 797 (2014), <https://doi.org/10.1088/2041-8205/797/2/L30>.
- [35] G. Mallocci, G. Mulas, C. Joblin, Electronic absorption spectra of PAHS up to vacuum UV: towards a detailed model of interstellar PAH photophysics, *Astron. Astrophys.* 426 (2004) 105–117, <https://doi.org/10.1051/0004-6361:20040541>.
- [36] G. Mallocci, G. Mulas, C. Cecchi-Pestellini, C. Joblin, Dehydrogenated polycyclic aromatic hydrocarbons and UV bump, *Astron. Astrophys.* 489 (2008) 1183–1187, <https://doi.org/10.1051/0004-6361:200810177>.
- [37] B. West, F. Useli-Bacchitta, H. Sabbah, V. Blanchet, A. Bodi, P.M. Mayer, C. Joblin, Photodissociation of pyrene cations: structure and energetics from C₁₆H₁₀⁺ to C₁₄⁺ and almost everything in between, *J. Phys. Chem. A* 118 (2014) 7824–7831, <https://doi.org/10.1021/jp506420u>.
- [38] M. Gatchell, H. Zettergren, Knockout driven reactions in complex molecules and their clusters, *J. Phys. B Atom. Mol. Opt. Phys.* 49 (2016), 162001, <https://doi.org/10.1088/0953-4075/49/16/162001>.
- [39] M.H. Stockett, H. Zettergren, L. Adoui, J.D. Alexander, U. Berziņš, T. Chen, M. Gatchell, N. Haag, B.A. Huber, P. Hvelplund, A. Johansson, H.A.B. Johansson, K. Kulyk, S. Rosén, P. Rousseau, K. Stöckel, H.T. Schmidt, H. Cederquist, Nonstatistical fragmentation of large molecules, *Phys. Rev.* 89 (2014), 032701, <https://doi.org/10.1103/PhysRevA.89.032701>.
- [40] B.J. West, L. Lesniak, P.M. Mayer, Why do large ionized polycyclic aromatic hydrocarbons not lose C₂H₂? *J. Phys. Chem. A* 123 (2019) 3569–3574, <https://doi.org/10.1021/acs.jpca.9b01879>.
- [41] P. Pla, C. Dubosq, M. Rapacioli, E. Posenitskiy, M. Alcamí, A. Simon, Hydrogenation of C₂₄ carbon clusters: structural diversity and energetic properties, *J. Phys. Chem. A* 125 (2021) 5273–5288.
- [42] D. Campisi, A. Candian, Do defects in PAHs promote catalytic activity in space? Stone–Wales pyrene as a test case, *Phys. Chem. Chem. Phys.* 22 (2020) 6738–6748, <https://doi.org/10.1039/C9CP06523G>.
- [43] G. Trinquier, A. Simon, M. Rapacioli, F.X. Gadéa, PAH chemistry at eV internal energies. 2. Ring alteration and dissociation, *Molecular Astrophysics* 7 (2017) 37–59, <https://doi.org/10.1016/j.molap.2017.02.002>.
- [44] O. Berné, A.G.G.M. Tielens, Formation of buckminsterfullerene (C₆₀) in interstellar space, *Proc. Natl. Acad. Sci. U. S. A* 109 (2012) 401–406, <https://doi.org/10.1073/pnas.1114207108>.
- [45] J. Zhen, S.R. Castillo, C. Joblin, G. Mulas, H. Sabbah, A. Giuliani, L. Nahon, S. Martin, J.-P. Champeaux, P.M. Mayer, VUV photo-processing of PAH cations: quantitative study on the ionization versus fragmentation processes, *Astrophys. J.* 822 (2016) 113, <https://doi.org/10.3847/0004-637X/822/2/113>.
- [46] G. Wenzel, C. Joblin, A. Giuliani, S. Rodriguez Castillo, G. Mulas, M. Ji, H. Sabbah, S. Quiroga, D. Peña, L. Nahon, Astrochemical relevance of VUV ionization of large PAH cations, *Astron. Astrophys.* 641 (2020) A98, <https://doi.org/10.1051/0004-6361/202038139>.
- [47] G. Reitsma, L. Boschman, M.J. Deuzeman, S. Hoekstra, R. Hoekstra, T. Schlathöler, Near edge X-ray absorption mass spectrometry on coronene, *J. Chem. Phys.* 142 (2015), 024308, <https://doi.org/10.1063/1.4905471>.
- [48] T. Monfredini, H.M. Quitián-Lara, F. Fantuzzi, W. Wolff, E. Mendoza, A.F. Lago, D.A. Sales, M.G. Pastoriza, H.M. Boechat-Roberty, Destruction and multiple ionization of PAHs by X-rays in circumnuclear regions of AGNs, *Mon. Not. Roy. Astron. Soc.* 488 (2019) 451–469, <https://doi.org/10.1093/mnras/stz1021>.
- [49] E.R. Micelotta, A.P. Jones, A.G.G.M. Tielens, Polycyclic aromatic hydrocarbon processing in interstellar shocks, *Astron. Astrophys.* 510 (2010) A36, <https://doi.org/10.1051/0004-6361/200911682>.
- [50] M. Gatchell, H. Zettergren, F. Seitz, T. Chen, J.D. Alexander, M.H. Stockett,

- H.T. Schmidt, A. Ławicki, J. Rangama, P. Rousseau, M. Capron, S. Maclot, R. Maisonnay, A. Domaracka, L. Adoui, A. Méry, J.-Y. Chesnel, B. Manil, B.A. Huber, H. Cederquist, Ions colliding with polycyclic aromatic hydrocarbon clusters, *Phys. Scripta* T156 (2013), 014062, <https://doi.org/10.1088/0031-8949/2013/T156/014062>.
- [51] G. Reitsma, H. Zettergren, L. Boschman, E. Bodewits, R. Hoekstra, T. Schlathöler, Ion–polycyclic aromatic hydrocarbon collisions: kinetic energy releases for specific fragmentation channels, *J. Phys. B Atom. Mol. Opt. Phys.* 46 (2013), 245201, <https://doi.org/10.1088/0953-4075/46/24/245201>.
- [52] F. Rico-Villas, J. Martín-Pintado, E. González-Alfonso, V.M. Rivilla, S. Martín, S. García-Burillo, I. Jiménez-Serra, M. Sánchez-García, Vibrationally excited HC₃N emission in NGC 1068: tracing the recent star formation in the starburst ring, *Mon. Not. Roy. Astron. Soc.* 502 (2021) 3021–3034, <https://doi.org/10.1093/mnras/stab197>.
- [53] K. Ferrière, Interstellar gas within ~10 pc of Sagittarius A *, *Astron. Astrophys.* 540 (2012) A50, <https://doi.org/10.1051/0004-6361/201117181>.
- [54] W. Lu, P. Kumar, N.J. Evans, Infrared emission from tidal disruption events – probing the pc-scale dust content around galactic nuclei, *Mon. Not. Roy. Astron. Soc.* 458 (2016) 575–581, <https://doi.org/10.1093/mnras/stw307>.
- [55] E.A. Rohlfing, D.M. Cox, A. Kaldor, Production and characterization of supersonic carbon cluster beams, *J. Chem. Phys.* 81 (1984) 3322–3330, <https://doi.org/10.1063/1.447994>.
- [56] E.B. Jochnowitz, J.P. Maier, Electronic spectroscopy of carbon chains, *Mol. Phys.* 106 (2008) 2093–2106, <https://doi.org/10.1080/00268970802208588>.
- [57] J.P. Maier, Electronic spectroscopy of carbon chains, *Chem. Soc. Rev.* 26 (1997) 21, <https://doi.org/10.1039/cs9972600021>.
- [58] T.F. Giesen, A. Van Orden, H.J. Hwang, R.S. Fellers, R.A. Provençal, R.J. Saykally, Infrared laser spectroscopy of the linear C₁₃ carbon cluster, *Science* 265 (1994) 756–759, <https://doi.org/10.1126/science.11539187>.
- [59] P. Neubauer-Guenther, T.F. Giesen, U. Berndt, G. Fuchs, G. Winnewisser, The Cologne Carbon Cluster Experiment: ro-vibrational spectroscopy on C₈ and other small carbon clusters, *Spectrochim. Acta Mol. Biomol. Spectrosc.* 59 (2003) 431–441, [https://doi.org/10.1016/S1386-1425\(02\)00380-3](https://doi.org/10.1016/S1386-1425(02)00380-3).
- [60] J.R. Heath, A. Van Orden, H.J. Hwang, E.W. Kuo, K. Tanaka, R.J. Saykally, Toward the detection of pure carbon clusters in the ISM, *Adv. Space Res.* 15 (1995) 25–33, [https://doi.org/10.1016/S0273-1177\(99\)80060-X](https://doi.org/10.1016/S0273-1177(99)80060-X).
- [61] T.F. Giesen, R. Gendriesch, F. Lewen, G. Winnewisser, Interstellar Detection of CCC and High-Precision Laboratory Measurements Near 2 THz, *Astrophys. J.* 551 (2001) L181, <https://doi.org/10.1086/320024>.
- [62] P.F. Bernath, K.H. Hinkle, J.J. Keady, Detection of C₅ in the circumstellar shell of IRC+10216, *Science* 244 (1989) 562–564, <https://doi.org/10.1126/science.244.4904.562>.
- [63] K.W. Hinkle, J.J. Keady, P.F. Bernath, Detection of C₃ in the circumstellar shell of IRC+10216, *Science* 241 (1988) 1319–1322, <https://doi.org/10.1126/science.241.4871.1319>.
- [64] J. Cernicharo, J.R. Goicoechea, E. Caux, Far-infrared detection of C₃ in Sagittarius B2 and IRC +10216, *Astrophys. J.* 534 (2000) L199–L202, <https://doi.org/10.1086/312668>.
- [65] S. Yang, K.J. Taylor, M.J. Craycraft, J. Conceicao, C.L. Pettiette, O. Cheshnovsky, R.E. Smalley, UPS of 2–30-atom carbon clusters: chains and rings, *Chem. Phys. Lett.* 144 (1988) 431–436, [https://doi.org/10.1016/0009-2614\(88\)87291-9](https://doi.org/10.1016/0009-2614(88)87291-9).
- [66] J. Hunter, J. Fye, M. Jarrold, Carbon rings, *J. Phys. Chem.* 97 (1993) 3460–3462, <https://doi.org/10.1021/j100116a003>.
- [67] J. Hunter, J. Fye, M. Jarrold, Annealing and dissociation of carbon rings, *J. Chem. Phys.* 99 (1993) 1785–1795, <https://doi.org/10.1063/1.465295>.
- [68] J.D. Presilla-Márquez, J.A. Sheehy, J.D. Mills, P.G. Carrick, C.W. Larson, Vibrational spectra of cyclic C₆ in solid argon, *Chem. Phys. Lett.* 274 (1997) 439–444, [https://doi.org/10.1016/S0009-2614\(97\)00700-8](https://doi.org/10.1016/S0009-2614(97)00700-8).
- [69] S.L. Wang, C.M.L. Rittby, W.R.M. Graham, Detection of cyclic carbon clusters. I. Isotopic study of the ν₄(e⁻) mode of cyclic C₆ in solid Ar, *J. Chem. Phys.* 107 (1997) 6032–6037, <https://doi.org/10.1063/1.475316>.
- [70] S.L. Wang, C.M.L. Rittby, W.R.M. Graham, Detection of cyclic carbon clusters. II. Isotopic study of the ν₁₂(eu) mode of cyclic C₈ in solid Ar, *J. Chem. Phys.* 107 (1997) 7025–7033, <https://doi.org/10.1063/1.474945>.
- [71] J.D. Presilla-Márquez, J. Harper, J.A. Sheehy, P.G. Carrick, C.W. Larson, Vibrational spectra of cyclic C₈ in solid argon, *Chem. Phys. Lett.* 300 (1999) 719–726, [https://doi.org/10.1016/S0009-2614\(98\)01409-2](https://doi.org/10.1016/S0009-2614(98)01409-2).
- [72] A.K. Ott, G.A. Rechtsteiner, C. Felix, O. Hampe, M.F. Jarrold, R.P. Van Duyne, K. Raghavachari, Raman spectra and calculated vibrational frequencies of size-selected C₁₆, C₁₈, and C₂₀ clusters, *J. Chem. Phys.* 109 (1998) 9652–9655, <https://doi.org/10.1063/1.477632>.
- [73] G.A. Rechtsteiner, C. Felix, A.K. Ott, O. Hampe, R.P. Van Duyne, M.F. Jarrold, K. Raghavachari, Raman and fluorescence spectra of size-selected, matrix-isolated C₁₄ and C₁₈ neutral carbon clusters, *J. Phys. Chem. A.* 105 (2001) 3029–3033, <https://doi.org/10.1021/jp003615r>.
- [74] M. Grutter, M. Wyss, E. Riplov, J.P. Maier, S.D. Peyerimhoff, M. Hanrath, Electronic absorption spectra of linear C₆, C₈ and cyclic C₁₀, C₁₂ in neon matrices, *J. Chem. Phys.* 111 (1999) 7397–7401, <https://doi.org/10.1063/1.480062>.
- [75] A.E. Boguslavskiy, H. Ding, J.P. Maier, Gas-phase electronic spectra of C₁₈ and C₂₂ rings, *J. Chem. Phys.* 123 (2005), 034305, <https://doi.org/10.1063/1.1961564>.
- [76] P.W. Fowler, N. Mizoguchi, D.E. Bean, R.W.A. Havenith, Double aromaticity and ring currents in all-carbon rings, *Chem. Eur. J.* 15 (2009) 6964–6972, <https://doi.org/10.1002/chem.200900322>.
- [77] J.T. Buntine, M.I. Cotter, U. Jacovella, C. Liu, P. Watkins, E. Carrascosa, J.N. Bull, L. Weston, G. Muller, M.S. Scholz, E.J. Bieske, Electronic spectra of positively charged carbon clusters—C_{2n}⁺ (n = 6–14), *J. Chem. Phys.* 155 (2021), 214302, <https://doi.org/10.1063/5.0070502>.
- [78] J. Rademacher, E. Reedy, E. Campbell, Electronic spectroscopy of monocyclic carbon ring cations for astrochemical consideration, *J. Phys. Chem. A.* 126 (2022), <https://doi.org/10.1021/acs.jpca.2c00650>.
- [79] S. Iida, W. Hu, R. Zhang, H. Tanuma, K. Masuhara, P. Ferrari, H. Shiromaru, T. Azuma, K. Hansen, Thermal radiative cooling of carbon cluster cations C_n⁺, N = 9, 11, 12, 17–27, *Mon. Not. Roy. Astron. Soc.* 514 (2022) 844–851, <https://doi.org/10.1093/mnras/stac1349>.
- [80] M.H. Stockett, J.N. Bull, J.T. Buntine, E. Carrascosa, M. Ji, N. Kono, H.T. Schmidt, H. Zettergren, Unimolecular fragmentation and radiative cooling of isolated PAH ions: a quantitative study, *J. Chem. Phys.* 153 (2020), 154303, <https://doi.org/10.1063/5.0027773>.
- [81] B. Zhu, J.N. Bull, M. Ji, H. Zettergren, M.H. Stockett, Radiative cooling rates of substituted PAH ions, *J. Chem. Phys.* 5 (2022), 0089687, <https://doi.org/10.1063/5.0089687>.